Very low-grade metamorphic study in the pre-Late Cretaceous terranes of New Caledonia (southwest Pacific Ocean)

Sébastien Potel

Very low-grade metamorphic study in the pre-Late Cretaceous terranes of New Caledonia (SW Pacific Ocean)

Short title: Low-grade metamorphism in New Caledonia

SÉBASTIEN POTEL [1, 2]

[1] Mineralogisch-Petrographisches Institut der Universität Basel, Bernoullistrasse 30, CH-4056 Basel, Switzerland

[2] present address: Institute of Geosciences, Department of Geology, Senckenberganlage 32-34, D-60054 Frankfurt am Main, Germany

s.potel@em.uni-frankfurt.de

Tel: ++49/(0) 641 99 36035

Fax: ++49/(0) 69 798 22958

ABSTRACT

Pre-Late Cretaceous terranes from the central part of New Caledonia have been metamorphosed under very low-grade conditions by two high-pressure/low-temperature events. This study investigates the metamorphic patterns using phyllosilicate crystallinities, electron microprobe analyses and petrography. The first metamorphic event is of Late Jurassic age and characterized by anchizonal to epizonal conditions and a decrease of KI and ÁI values from NE towards SW. This trend is also confirmed by chlorite thermometry. In the south of the area, un-metamorphosed sediments (diagenetical KI values) are observed in the Senonian "formation à charbons", postdating the metamorphism in this region.

The second metamorphism is an Eocene HP event, which overprints the Late Jurassic metamorphism in the northern part of the studied area. In this zone, the pattern of KI and ÁI indicates another gradient with increasing metamorphic conditions from SW towards NE. Temperatures calculated by chlorite thermometry also indicate an evolution from SW towards NE with increase of temperature from 298 ± 8°C to 327 ± 16°C.

In both metamorphic zones, the K-white mica *b* cell dimension calculated on micas analyzed at electron microprobe are in good agreement with high-pressure/low-temperature metamorphic conditions (b_0 > 9.04 Å). A combination of chlorite thermometry and K-white mica *b* cell dimension allows to estimate a minimum pressure of 1.3 GPa in the Eocene zone (in excellent agreement with the 1.5 GPa registered in the northern part of New Caledonia) and a minimum of 1.1 GPa in the Late Jurassic metamorphic part.

Key words: phyllosilicates, illite crystallinity, New Caledonia, very low-grade metamorphism, hig-pressure/low-temperature.

INTRODUCTION

Since the first study by Brothers (1970), New Caledonia has been well known for its Eocene high-pressure (HP) metamorphic belt located in the northern part of the island. This Eocene metamorphism has been the subject of numerous petrological studies (Brothers, 1970; Brothers & Black, 1973; Black & Brothers, 1977; Diessel et al., 1978; Brothers & Yokohama, 1982; Ghent et al., 1987; Black et al., 1993; Cluzel et al., 1994; Clarke et al., 1997; Carson et al., 2000; Fitzherbert et al., 2003), showing an increase of grade toward the NE with an evolution from prehnite-pumpellyite- to eclogite-facies. A recent low-grade metamorphic study (Potel et al., 2006) characterized through a multi-method investigation of phyllosilicates, fluid inclusion and organic matter the metamorphic phyllosilicate evolution in the Eocene HP metamorphic belt.

Less well studied are the pre-Late Cretaceous terranes in the central part of New Caledonia. Routhier (1953) distinguished two events: one Pre-Permian (high pressure/low temperature) and one post Jurassic and pre-Senonian (greenschist facies). Guérangé et al. (1973) demonstrated that the second metamorphic event locally reached blueschist facies. Paris (1981) reinterpreted the second event as being a sub-greenschist to greenschist facies and associated the presence of lawsonite to a local increase of the pressure in the vicinity of fault zones. A recent study by Cluzel & Meffre (2002) demonstrated that the “pre-Permian basement” (pre-Late Cretaceous terranes) was of Jurassic age and only affected by a Late Jurassic HP metamorphism (ca 150 Ma). The main problem remains to differentiate and to characterize the metamorphism in the region due to the presence of the same index minerals in the Eocene belt and in the Central Chain, together with the scarcity of index minerals in the Central Chain.

In low-temperature/high-pressure (LT/HP) metamorphic belt, the characterization of metamorphic conditions is difficult. Only metabasites or Al-rich metapelites will develop the indicative index minerals. The common mineral assemblage in metapelites is essentially composed of quartz, illite/muscovite and chlorite. Therefore the study of reaction progress and development of clay minerals are useful tools to describe the thermal and barometric evolution during metamorphism. In the case of poly-metamorphic areas, the characterization of phyllosilicates is the only method to decipher the metamorphic zonation.

The aim of this paper is to present the results of the first investigation of the very low-grade metapelites in the Central Chain, using the phyllosilicate crystallinities, chlorite thermometry and *b* cell dimensions of K-white micas. These data should help us to decipher the different metamorphic zonation and gradients in the central part of New Caledonia. Therefore, the results are compared with the existing data set obtained by Potel et al. (2006) in the Eocene HP metamorphic belt.

REGIONAL GEOLOGY

New Caledonia is a dispersed fragment of the eastern margin of Gondwana resulting from the opening of the Tasman Sea by rifting of New Caledonia and New Zealand from Australia. In Late Eocene time, the New Caledonian fragment collided with an intraoceanic island-arc system (Cluzel et al., 1994; Aitchison et al., 1995; Clarke et al., 1997; Cluzel et al., 2001), and a NE-dipping subduction system was established beneath the Loyalty Basin. The collision, responsible for the main deformation of the continental basement of New Caledonia, generated a HP schist belt coeval with the southwestwards thrusting of two nappes over the basement: the Poya nappe or

"formation des basalts" (Paris, 1981) (a mafic sheet comprising dolerite, tectonized tholeiitic pillow basalts and abyssal argillites) and the peridotite nappe (an ophiolite complex) (Fig. 1). The basement is composed of terranes of Paleozoic to Mesozoic age of varying metamorphic grade, transgressively overlain by upper Cretaceous to Eocene sedimentary rocks deposited during Gondwana dispersal (Aitchison et al., 1995; Clarke et al., 1997). The basement is affected by Late Jurassic high-pressure metamorphism (ca 150 Ma, Cluzel & Meffre, 2002). The late Eocene HP metamorphism observed in the northern part of New Caledonia overprinted the northern part of these terranes (Cluzel et al., 2001). The Late pre-Cretaceous terranes (basement) comprised (Fig. 1): (1) the "*Boghen terrane*", an accretionary complex formed during the Jurassic period along the East-Gondwana active margin (Cluzel & Meffre, 2002) is a metamorphosed volcano-sedimentary pile composed of pillow basalt, radiolarian chert, mafic and felsic tuffs and minor carbonatic sediments (Cluzel, 1996); (2) the *"Central Chain terrane"*, volcano-sedimentary arc terrane of mid-Triassic to late Jurassic age (Meffre, 1995); (3) the "*Koh terrane ophiolites*", a dismembered Late Carboniferous fore-arc ophiolite (Aitchison et al., 1998); (4) the "*Téremba-Moindou terrane*" of Permian- to Late Jurassic age, composed of volcano-sedimentary rocks (Aitchison et al., 1998). A transgressive sequence of Upper Cretaceous (Late Cenomanian to Late Eocene) coal measures and conglomerates ("formation à charbon"; Paris, 1981) overlies the late pre-Cretaceous basement with angular unconformities. This unit provides a minimum age for the timing of amalgamation of New Caledonia basement terranes to Gondwana (Aitchison et al., 1998).

MATERIALS AND METHODS

This study is focused on the Central Chain and Boghen terranes and the "Formation à charbon" (Fig. 1). Samples for this study were collected from 86 localities (Table 1) in the Central Chain (53) and Boghen (16) terranes and in the "formation à charbon" (17). In New Caledonia, outcrops are poor due to extensive tropical weathering, limiting the availability of fresh samples mainly to road cuts. In many common rocks, such as marine pelites and carbonates rocks, no diagnostic minerals and mineral assemblages form in the very low-grade field. In these rocks, the transitions from non-metamorphic to very low-grade and from very low-grade to low-grade metamorphic domains take place through the diagenetic zone, the anchizone and the epizone, each zone being characterized by specific values of the illite Kübler Index (KI) (Árkai et al. 2003).

CLAY MINERAL ANALYSIS

Clay mineral separation was conducted using techniques described by Schmidt et al. (1997). For the XRD analyses of ≤2μm fractions, oriented samples, which were air-dried, solvated with ethylene glycol and heated (550°C) were prepared. Illite and chlorite crystallinity was measured on air-dried and glycolated samples using a D5000 Bruker-AXS (Siemens) diffractometer, CuKα radiation at 40 kV & 30 mA and automatic divergence slits (primary and secondary V20) with a secondary graphite monochromator. Illite crystallinity was calculated using the software DIFFRAC^{Plus} TOPAS (by ©Bruker AXS). The illite crystallinity index is defined as the full width at half maximum (FWHM) intensity of the first illite-muscovite basal reflection (10 Å) and expressed in Δ°2Θ (Kübler, 1968). Illite crystallinity values were transformed into Kübler index values using a correlation with the standard samples of Warr & Rice

(1994) (**KI_{CIS} = 1.343 * IC_{Basel} – 0.003**). The Kübler index was used to define the limits of metamorphic zones, and the transition values were chosen as follows: KI = 0.25 Δ°2Θ for the epizone to high anchizone boundary, KI = 0.30 Δ°2Θ for the high to low anchizone boundary and KI = 0.42 Δ°2Θ for the low anchizone to diagenetic zone. The same experimental conditions were also used to determine chlorite crystallinity on the (002) peak, where (ChC(002)) corresponds to the full width at half maximum intensity values of the second (7 Å) basal reflection of chlorite. The ChC(002) measurements were calibrated with those of Warr & Rice (1994) and expressed as the Árkai index (ÁI) (Guggenheim et al., 2002): **ÁI = 0.766 * ChC(002) + 0.117**. The anchizone boundaries for the Árkai index were defined by correlation with the Kübler index and are given as 0.24 Δ°2Θ for the epizone to anchizone boundary and 0.30 Δ°2Θ for the anchizone to diagenetic zone.

MINERAL CHEMISTRY

Mineral compositions in the metapelites were determined by electron probe microanalysis using a JEOL JXA-8600 superprobe at the University of Basel with four wavelength dispersive spectrometers, equipped with Voyager software by NORAN instruments. A ZAF-type correction procedure was used for all data reduction and all Fe was assumed to be ferrous. In order to avoid volatilization of light elements, low-grade metamorphic minerals were analyzed using a 10 nA beam current, an accelerating voltage of 15 kV, an acquisition time of 10 or 20 seconds, rastered over an area of 26 μm^2. The standards used for the different elements were as follows: olivine for Si and Mg; rutile for Ti; gehlenite for Al; graftonite for Mn and Fe; wollastonite for Ca; albite for Na; and orthoclase for K.

RESULTS

MINERALOGY

The mineralogy of the studied samples is given in Table 1. Mineral abbreviations are those of Kretz (1983). Pelites, tuffs and metamarls were analyzed. In Figure 2, the distribution of the index minerals lawsonite, glaucophane and stilpnomelane is represented.

The meta-marls were sampled in the three units. Generally, the mineral assemblages consist of Qtz + K-white mica + Chl + Ab + Cal. In the Boghen terrane, Ep and Gln are present in addition, and in the Central Chain terrane Stp is also observed (Fig. 2). In their <2 μm grain-size fraction, illite-muscovite predominates in association with Chl and quartz. Albite is only present in minor amounts.

In the metapelites, the mineral assemblages consist of Qtz, K-white mica, Chl and/or Kln with minor amounts of mixed-layer minerals (I/S, C/S and Kaolinite/Smectite (K/S)), Ab, and index minerals depending on the metamorphic grade (stilpnomelane, lawsonite, glaucophane) (Fig. 2). In their <2 μm fractions, illite-muscovite or phengitic muscovite predominate in the higher-grade samples. Discrete paragonite is also found in minor quantities and margarite is observed in sample MF3100.

In the Central Chain terrane, the meta-tuffs were sampled in the region of Touho. Their mineral assemblages are composed of Qtz + Ab + Chl + K-white mica ± Stp (Fig. 2). The <2μm grain-size fraction is dominated by illite-muscovite and chlorite.

Figure 3 shows the distribution of the illite crystallinity (KI data). The FWHM values are presented in Table 1.

In the Central Chain terrane, metamorphic values range between high anchizone and epizone (Table 1, Fig. 4a). A peak in the distribution of KI-values is observed at epizonal values (Fig. 4a). The highest KI value (sample MF3110) is due to the presence of discrete paragonite in great amount, leading to a broad 10Å peak.

In the Boghen terrane the KI was determined on 15 samples (Fig. 4b). All of these samples yield epizonal metamorphic conditions (Fig. 4b) (Table 1).

The 16 KI values from the "formation à charbon" range from epizone to low diagenesis (Table 1 and Fig. 4c). Samples from the south are lower metamorphosed with only diagenetical conditions (Fig. 3). A trend of increasing grade from low anchizone to high anchizone (limit epizone, sample MF3080) is observed in the region between Poindimié and Ponérihouen (Fig. 3).

A significant positive linear correlation ($r^2 = 0.65$) is found between Kübler and Árkai indices (Fig. 5), rending greater reliability to the metamorphic grade estimate deduced from KI values, which can be hindered by broadening of the reflectance peak due to the presence of discrete paragonite. Overall, the pattern of very low-grade metamorphism revealed by the chlorite crystallinity (Fig. 6) agrees well with the pattern of the illite crystallinity (Fig. 3). No diagenetic ÁI values are observed due to the presence of kaolinite in samples where diagenetical KI values were measured.

In northern New Caledonia, Potel et al. (2006) deduced temperature limits for anchizone based on oxygen isotopic thermometry. The anchizone is bracketed between $230 \pm 10°C$ and $295 \pm 10°C$, which is in good agreement with the approximate boundary found in the literature. Consequently, temperature estimates for the

investigated samples ranged between ca. 230 and 350°C (0.16 < KI < 0.42 Δ°2Θ). Only in south of the "formation à charbon", the temperatures were lower than 230°C (KI > 0.42 Δ°2Θ).

Mineral chemistry

Due to the small grain size of the phyllosilicates, special care was taken to differentiate between detrital and newly formed metamorphic grains.

Representative compositions of K-white mica are listed in Table 2. Mica analyses showing more than 0.5% (MnO %+ TiO_2 %) were rejected (Vidal & Parra, 2000). In a Si-Al_{tot} diagram (Fig. 7a), the analyses show a significant deviation from the Tschermak exchange line. Considering the analyses reported in Table 2, the total interlayer charge (t.i.c. = Ca+Na+2K) is between 1.00 and 0.94, except for sample PS46b, where a Prl substitution could be assumed (Figs. 7a & 7d) in addition to the Tschermark's substitution. Additional substitutions are required to explain the excess of Fe and Mg in samples PS54, PS56b, PS69, PS85 (Figs. 7a & 7b). The excess of Mg+Fe could be explained by a di/trioctahedral substitution common in dioctahedral micas (Vidal & Parra, 2000; Parra et al., 2002). Figure 7c shows a correlation between the Fe and Mg contents in the individual samples (probably dependant on the bulk composition) except for samples PS46b. On the basis of model calculations supposing various mixtures (Fig. 7b), no contamination of the analyses by quartz or chlorite has occurred.

In Figure 7d, the K-white mica analyses fall in a cluster between the muscovite-phengite and the muscovite-illite lines, indicating a small deficit in t.i.c. (values range

between 0.85 and 1.00 p.f.u.). Figure 7e shows that the Na content of K-white mica is very low and thus the *b* cell dimension is not influenced by K-Na exchange. Therefore use of the *b* cell dimension should be accurate (Guidotti et al., 1989).

Although the number of data pairs is relatively low (n = 5), we investigated the relation between the metamorphic grade of our samples with the chemistry of the K-white micas. Figure 7f reveals no obvious correlation between KI values and Si content. This indicates the occurrence of other substitutions in addition to the celadonitic one, probably the di/trioctahedral substitution previously discussed.

The Na/(Na+K) ratios are lower than 0.15 in the analyzed samples permitting to calculate K-white mica b cell dimension parameters using the regression equations from Guidotti et al. (1989). Kisch et al. (2006) outlined the possibility to overestimate or underestimate the b_0 in the case of Fe-free Phengite or Fe-rich celadonite. Here, the Fe^{2+}/(Si-6) ratio is in the range where the regression equations can reasonably used and this up to ca. 3.55 Si p.f.u..

Compositions of chlorite are normalized to 28 oxygens (Table 3) and fulfill the criterion of non contamination, ∑Ca+Na+K < 0.2 (Dalla Torre et al., 1996). Using the classification of Zane & Weiss (1998), chlorites in the studied samples are trioctahedral type I where ($X_{Mg} + X_{Fe} \geq X_{Al} + X_{vacancy}$). X_{Mg} varies between 0.37 and 0.93, and according to Hey (1954), the chlorites lie mainly in the ripidolite, pichnochlore and brunsvigite fields.

The low total interlayer charge of the chlorites (<0.2 p.f.u.) indicates that smectite or illite impurities are insignificant (Fig. 8a). The increase of (Al^{VI}-Al^{IV}) could be attributed to increasing sudoitic substitution (di-trioctahedral) (Árkai et al., 2003). Correlations observed for apparent octahedral vacancies with (Al^{VI}-Al^{IV}) (Fig. 8b) and

apparent octahedral vacancies with sum of octahedral divalent cations (Fig. 8c) prove the sudoitic substitution in the analyzed chlorites. Figure 8d demonstrates that, in addition to the Tschermak substitution, the di-trioctahedral substitution plays an important role in chlorites.

Using the chlorite-Al^{IV} thermometer of Cathelineau (1988), we calculated mean T values between 266 and 327°C (Table 3). These temperatures are in good agreement with those deduced from the KI values.

Based on Ramírez & Sassi (2001), the temperature derived from the chlorite and the K-white b cell dimension values are used to estimate the P conditions in samples PS56b and PS46b. In Figure 9, pressure can be estimated around 1.1 GPa for PS46b and 1.3 GPa for PS56b. In comparison, we give the P and T conditions obtained in the glaucophane zone of the Eocene HP metamorphic belt (up to 1.5 GPa and 410°C; Potel et al., 2006).

DISCUSSION

Mineral assemblages observed in the studied samples are compatible with the mineral boundary drawn by Paris (1981) (Fig. 2). Lawsonite and stilpnomelane are observed in the Central Chain terrane, in the region of Poindimié and in the southern part of the studied area. In the region of Poindimié, lawsonite is also present in the "formation à charbon". Glaucophane minerals are found in samples from the Boghen terrane in the region of the "col des Roussettes".

The metamorphic conditions observed by the illite and chlorite crystallinity are very similar to those indicated by the mineral facies. In the lawsonite Eocene zone (Figs. 3 & 6), the metamorphic conditions indicated by the phyllosilicates crystallinity

(KI and ÁI) are in good agreement with those observed in the Eocene HP belt to the north (Potel et al., 2006). The KI values indicate epizonal conditions, except in the "formation à charbon" where values are anchizonal (but still compatible with the lawsonite occurrence). There, an increasing metamorphic gradient from south to north is observed (Fig. 3).

In the south of the studied area, the "formation à charbon" reaches only diagenetical conditions (IC $\geq$ 0.42 $\Delta°2\Theta$) and kaolinite is present in all samples, contrasting with higher metamorphic conditions in the Boghen and Central Chain terranes. In the profile 2 (Figs. 2 & 10), metamorphic contrast between "formation à charbon" and Central Chain terrane is observed with the presence of diagenetical samples in the proximity of epizonal ones. An increasing metamorphic gradient can be observed with a decrease of the KI and ÁI values in the Boghen terrane from NE towards SW (profile 1, Figs. 2 & 10). Due to the lack of samples in the Central Chain this gradient cannot clearly observed. An increase of the values in the middle of the Boghen terrane could be explained by the presence of a thrust fault. In profile 2 (Fig. 10) due to the low density of the sample (only two samples), the trend in each terrane is not so clear with an apparent metamorphic inversion in the Chain Central terrane and an iso-metamorphism in the Boghen terrane. However, the phyllosilicate crystallinities are in good agreement with the previous metamorphic studies based on mineral assemblages, indicating an increasing of metamorphism from NE toward SW (Cluzel & Meffre, 2002). In the north of the studied area (Central Chain terrane), metamorphic conditions reach anchizone (Fig. 3) with the presence of stilpnomelane (no lawsonite was observed, Fig. 2).

Overall in the studied area, K-white *b* cell dimensions (Table 2) range between 9.04 and 9.05 Å indicating high-pressure conditions (Merriman & Peacor, 1999). However, different metamorphic evolution can be observed. In the Eocene lawsonite zone, it is observed that the temperature (chlorite thermometry) is higher along the eastern coast as to the west. Moreover, in the "formation à charbon" another gradient is observed with increase of metamorphic conditions from S to N as indicated by illite crystallinity. These observations lead to the definition in the Eocene lawsonite zone of a metamorphic gradient increasing from SW towards NE (Fig. 11), like in the northern part of New Caledonia (Potel et al., 2006). In the Nimbaye Valley (Fig. 11), south of the Eocene lawsonite zone, the chlorite thermometry indicates higher temperature (T = 312 ± 12°C, PS46b) than northern in Eocene (T = 298 ± 8°C, MF3100). In this Valley, we observed an increase of metamorphic grade (decrease of the KI and ÁI values) from NE towards SW, i.e. inverse to the gradient observed in the Eocene Zone. Based on all these results, an approximate limit between the Eocene metamorphism and the Late Jurassic metamorphism can be drawn (Fig. 11), similar to that drawn by Cluzel et al. (2001).

The metamorphic pattern revealed by the study of the phyllosilicate is compatible with the model given for the evolution of the central New Caledonia. The diagenetic values observed in the "formation à charbon" (Senonian age?) in the south confirmed the Pre-Late Cretaceous age of the metamorphism in this region (150 Ma, K-Ar on Glaucophane, Blake & Brothers (1977)). This metamorphism is of high-pressure type (K-white *b* cell dimensions higher than 9.04 Å) with an increasing gradient from NE towards SW. The later Eocene metamorphism affected only the north of the central area, leading to the drawn of an approximate limit based on the

metamorphism observed in the “formation à charbon” and the temperature values calculated on chlorite. The increase in metamorphic grade from SW to NE within this region is similar to that observed in the north of New Caledonia (Potel et al., 2006). The Touho fault (a dextral strike slip fault) separates this region from the late Eocene formation (Fig. 11, Cluzel et al., 2001) and moved it in its actual position.

AKNOWLEDGMENENTS

This research was supported by grant 50-506842.99 of the Swiss National Foundation. Prof. W. Franke and M. P. Doublier are thanked for their help in the correction of the manuscript.

REFERENCES

AITCHISON J. C., CLARKE G. L., MEFFRE S. & CLUZEL D. 1995. Eocene arc-continent collision in New Caledonia and implications for regional southwest Pacific tectonic evolution. *Geology* **23**, 161-164.

AITCHISON J. C., IRELAND T. R., CLARKE G. L., CLUZEL D., DAVIS A. M. & MEFFRE S. 1998. Regional implications of U/Pb SHRIMP age constraints on the tectonic evolution of New Caledonia. *Tectonophysics* **299,** 333-343.

ÁRKAI P., FARYAD S. W., VIDAL O. & BALOGH K. 2003. Very low-grade metamorphism of sedimentary rocks of the Meliata unit, Western Carpathians, Slovakia: implications of phyllosilicate characteristics. *International Journal of Earth Sciences* **92**, 68-85.

BLACK P. M. & BROTHERS R. N. 1977. Blueschist Ophiolites in the Melange Zone, Northern New Caledonia. *Contributions to Mineralogy and Petrology* **65**, 69-78.

CARSON C. J., CLARKE G. L. & POWELL R. 2000. Hydration of eclogite, Pam Peninsula, New Caledonia. *Journal of Metamorphic Geology* **18**, 79-90.

BLACK P. M., MAURIZOT P., GHENT E. D. & STOUT M. Z. 1993. Mg-Fe carpholites from aluminous schists in the Diahot region and implications for preservation of high-pressure/low-temperature schists, northern New Caledonia. *Journal of Metamorphic Geology* **11**, 455-460.

BROTHERS R. N. 1970. Lawsonite-Albite Schists from Northernmost New Caledonia. *Contributions to Mineralogy and Petrology* **25**, 185-202.

BROTHERS R. N. & BLACK Jr. M. C. 1973. Tertiary plate tectonics and high-pressure metamorphism in New Caledonia. *Tectonophysics* **17**, 337-358.

BROTHERS R. N. & YOKOYAMA K. 1982. Comparaison of the High-Pressure Schist Belts of New Caledonia and Sanbagawa, Japan. *Contributions to Mineralogy and Petrology* **79**, 219-229.

CATHELINEAU M. 1988. Cation site occupancy in chlorites and illites as a function of temperature. *Clay Minerals* **23**, 471-485.

CLARKE G. L., AITCHISON J. C. & CLUZEL D. 1997. Eclogites and blueschists of the Pam Peninsula, NE New Caledonia: a reappraisal. *Journal of Petrology* **38**, 843-876.

CLUZEL D. 1996. Affinités intra-océaniques des métavolcanites de l'unité de la Boghen (ex-Anté-Permien de Nouvelle-Calédonie, Pacifiue sud-ouest). Conséquences paleogéographiques. *Comptes Rendus Académie des Sciences Paris* **323**, 657-664.

CLUZEL D., AITCHISON J., CLARKE G., MEFFRE S. & PICARD C. 1994. Point de vue sur l'évolution tectonique et géodynamique de la Nouvelle-Calédonie (Pacifique, France). *Comptes Rendus Académie des Sciences Paris* **319**, 683-690.

CLUZEL D., AITCHISON J. C. & PICARD C. 2001. Tectonic accretion and underplating of mafic terranes in the Late Eocene intraoceanic fore-arc of New Caledonia (Southwest Pacific): geodynamic implications. *Tectonophysics* **340**, 23-59.

CLUZEL D. & MEFFRE S. 2002. L'unité de la Boghen (Nouvelle-Calédonie, Pacifique sud-ouest) : un complexe d'accrétion jurassique. Données radiochronologiques preliminaries U-Pb sur les zircons détritiques. *Comptes rendus des Géoscicences* **334**, 867-874.

DALLA TORRE M., LIVI K. J. T. & FREY M. 1996. Chlorites textures and composition from high pressure/low temperature metashales and metagraywackes, Franciscan complex, Diablo Range, California, U.S.A.. *European Journal of Mineralogy* **8**, 825-846.

DIESSEL C. F. K., BROTHERS R. N. & BLACK P. M. 1978. Coalification and Graphitization in High-Pressure Schists in New Caledonia. *Contributions to Mineralogy and Petrology* **68**, 63-78.

FITZHERBERT J. A., CLARKE G. L. & POWELL R. 2003. Lawsonite-omphacite-bearing metabasites of the Pam Peninsula, NE New Caledonia: Evidence for disrupted blueschist- to eclogite-facies conditions. *Journal of Petrology* **44**, 1805-1831.

GHENT,E. D., STOUT M., BLACK P. M. & BROTHERS R. N. 1987. Chloritoid-bearing rocks associated with blueschists and eclogites, northern New Caledonia. *Journal of Metamorphic Geology* **5**, 239-254.

GUÉRANGÉ B., LILLE B. & LOZES J. 1973. Données nouvelles concernant la stratigraphie, la sédimentologie, la pétrologie et la structure de la chaîne centrale de la Nouvelle-Calédonie. *Bulletin du BRGM Français* **2**, 127-137.

GUIDOTTI C. V., SASSI F. P. & BLENCOE J. G. 1989. Compositional controls on the *a* and *b* cell dimensions of 2M1 Muscovites. *European Journal of Mineralogy* **1**, 71-84.

GUGGENHEIM S. Jr., BAIN D. C., BERGAYA F., BRIGATTI M. F., DRITS V. A., EBERL D. D. et al. 2002. Report of the association internationale pour l'étude des argiles (AIPEA) nomenclature committee for 2001: order, disorder and crystallinity in phyllosilicates and the use of the "crystallinity index". *Clays and Clay Minerals* **50**, 406-409.

HEY M. H. 1954. A new review of the chlorites. *Mineralogical Magazine* **30**, 277-292.

KISCH H. J., SASSI R. & SASSI F. P. 2006. The *b0* lattice parameter and chemistry of phengites from HP/LT metapelites. *European Journal of Mineralgy* **18**, 207-222.

KRETZ,R. 1983. Symbols for rock-forming minerals. *American Mineralogist* **68**, 277-279.

KÜBLER B. 1968. Evaluation quantitative du métamorphisme par la cristallinité de l'illite. Etat des progrès réalisés ces dernières années. *Bulletin Centre Recherche Pau*, *S.N.P.A* **2**, 385-397.

MAURIZOT P., EBERLÉ J.-M., HABAULT C. & TESSAROLLO C. 1989. Carte géologique à l'échelle du 1/50 000, feuille Pam-ouégoa. (Map sheet and explanatory notes) Paris: BRGM, 81 pp.

MEFFRE S. 1995. The development of arc-related ophiolites and sedimentary sequences in New Caledonia. *PhD thesis*, University of Sydney, 236 pp.

MERRIMAN, R. J. & PEACOR, D. R. (1999). Very low-grade metapelites: mineralogy, microfabrics and measuring reaction progress. In: Frey, M. & Robinson, D. (eds.) *Low-grade metamorphism*. Blackwell Science, Oxford, 10-60.

PARIS J. P. 1981. Géologie de la Nouvelle-Calédonie, un essai de synthèse. Bureau de Recherches Géologiques et minières, 240 pp.

PARRA T., VIDAL O. & AGARD P. 2002. A thermodynamic model for Fe-Mg dioctahedral K white micas using data from phase-equilibrium experiments and natural peletic assemblages. *Contributions to Mineralogy and Petrology* **143**, 706-732.

POTEL S., FERREIRO MÄHLMANN R., STERN W., MULLIS J. & FREY M. 2006. Very low-grade metamorphic evolution of pelitic rocks under high-pressure/low-temperature conditions, NW New Caledonia (SW Pacific). *Journal of Petrology* **47**, 991-1015.

RAMÍREZ E. & SASSI R. 2001. The baric character of the Patagonian basement as deduced from the muscovite $d_{060,331}$ spacing: a first contribution from Eastern Andean Metamorphic Complex (Andes, Chile). *European Journal of Mineralogy* **13**, 1119-1126.

ROUTHIER P. 1953. Etude géologique du versant occidental de la Nouvelle-Calédonie entre le col de Boghen et la pointe d'Arama. *Mémoire de la Société Géologique Française* **32**, 1-127.

SCHMIDT D., SCHMIDT S. Th., MULLIS J., FERREIRO MÄHLMANN R. & FREY M. 1997. Very low grade metamorphism of the Taveyanne formation of western Switzerland. *Contributions to Mineralogy and Petrology* **129**, 385-403.

VIDAL O. & PARRA T. 2000. Exhumation paths of high-pressure metapelites obtained from local equilibria for chlorite-phengite assemblages. *Geological Journal* **35**, 139-161.

WARR L. N. & RICE A. H. 1994. Interlaboratory standardization and calibration of clay mineral crystallinity and crystallite size data. *Journal of Metamorphic Geology* **12**, 141-152.

ZANE A. & WEISS Z. 1998. A procedure for classifying rock-forming chlorites based on microprobe data. *Rendiconti Lincei Scienze Fisiche e Naturali* **9**, 51-56.

Fig. 1: Structural map of New Caledonia showing the major tectonic units (after Cluzel et al., 1994, Fitzherbert et al., 2003). The inset shows the location of New Caledonia in the southwest Pacific.

Fig. 2: Distribution of index minerals (Glaucophane, lawsonite and Fe-stilpnomelane) in the studied area. The Peridotites and Poya Nappes are coloured in black and the formation à charbon in light grey. Profiles 1 and 2 of Figure 10 are indicated in black.

Fig. 3: Distribution of Kübler index (KI) values in the studied area. The Peridotites and Poya Nappes are coloured in black and the formation à charbon in light grey.

Fig. 4: Histograms of illite crystallinity (KI) in the different terranes. (a) Central Chain terrane. (b) Boghen terrane. (c) "Formation à charbon".

Fig. 5: Correlation between KI (10Å) and ÁI (7Å) values. n = 46.

Fig. 6: Distribution of Árkai index (ÁI) values in the studied area. The Peridotites and Poya Nappes are coloured in black and the formation à charbon in light grey.

Fig. 7: (a-e) Compositional relations of metamorphic dioctahedral white micas. Cation numbers and ratios are calculated from electron microprobe analyses. t.i.c. = total interlayer charge = K+Na+2Ca per formula unit. (f) Relations between illite crystallinity (KI) and the chemistry of white mica.

Fig. 8: (a-d) Compositional variation of chlorite. Cation numbers and ratios are calculated from electron microprobe analyses. (a**)** t.i.c. (= total interlayer charge = K+Na+2Ca per formula unit) versus Al^{VI}-Al^{IV}. (b) Apparent octahedral vacancy (= 20-∑octahedral cations per formula unit) versus Al^{VI}-Al^{IV}. (c) Apparent octahedral vacancy versus total oct. R^{2+} (= Fe^{2+}+Mg^{2+}). (d) Al^{VI}+2Ti versus Al^{IV}. Arrows show trends of TK (Tschermak's), and AM (dioctahedral) substitutions, where $\Delta=Al^{IV}-(Al^{VI}+2Ti)$.

Fig. 9: Pressure-temperature conditions for samples PS46b and PS56b using K-white micas *b* cell dimension values and calculated chlorite temperature (after Cathelineau, 1988). In comparison, the stability field of sample MF3031 (cross hatched area) of the HP Eocene belt is represented (Potel et al., 2006). Iso K-white micas *b* cell dimension curves (dashed lines) are taken from Ramírez & Sassi (2001).

Fig. 10: Schematic cross-sections along two profiles (Fig. 2). Average values of Kübler index (KI) are indicated in bold and average values of Árkai Index (ÁI) in italic. Mineral abbreviations are those of Kretz (1983).

Fig. 11: Schematic geological map, the Peridotites and Poya Nappes are coloured in black and the formation à charbon in light grey. Chlorite temperature (after Cathelineau, 1988) and K-white micas *b* cell dimension values are indicated for the samples where it was calculated. Arrows indicate the metamorphic gradients (Eocene = A; Late Jurassic = B) observed in the different zones. The deduced limit of the Eocene HP metamorphism is represented with a bold grey line.

Table 1: Geographical location, rock type and mineralogy of the studied samples. FWHM and ChC(002) data of the studied samples.

Sample	Latitude	Longitude	Alt in m.	Rock type	Qtz	Ab	Ms	Chl	Pg	Kln	Stp	ML	others	Terrane	IC	ÁI
MF3077	20°56'10"	165°21'10"	20	pelite	*	*		*				C/S	Lws	F. charbon	-	0.17
MF3078	20°56'10"	165°21'00"	20	pelite	*		*	*	*					F. charbon	0.20	-
MF3080	21°00'15"	165°24'00"	40	pelite	*	*	*	*				C/S	Lws	F. charbon	0.20	-
MF3081	21°00'50"	165°22'50"	10	pelite	*	*	*	*	*				Lws	F. charbon	0.26	0.16
MF3082	21°00'21"	165°20'51"	40	pelite	*		*	*	*					Cent. Chain	0.24	0.21
MF3083	21°01'32"	165°23'10"	20	pelite	*	*	*		*	*				F. charbon	0.23	Kln
MF3085	21°02'29"	165°23'52"	20	pelite	*	*	*		*		*			F. charbon	0.23	-
MF3086	21°02'45"	165°23'19"	20	marl	*	*	*	*					Cal	F. charbon	0.13	0.19
MF3087	21°02'45"	165°23'59"	20	marl	*	*	*	*					Cal	F. charbon	0.10	0.14
MF3088	21°04'20"	165°24'50"	5	pelite	*	*	*		*	*				F. charbon	0.27	Kln
MF3089	21°05'12"	165°25'40"	5	pelite	*	*	*		*	*		K/S		F. charbon	0.27	Kln
MF3090	21°08'51"	165°28'11"	5	pelite	*	*	*	*						Cent. Chain	0.11	0.18
MF3098	20°58'38"	165°11'21"	40	pelite	*	*	*	*	*			C/S	Lws	Cent. Chain	0.18	-
MF3099	20°58'20"	165°11'53"	30	pelite	*	*	*	*						Cent. Chain	0.17	0.16
MF3100	20°57'45"	165°13'48"	20	pelite		*		*					Mrg+Ep	Cent. Chain	-	0.17
MF3101	20°58'22"	165°10'51"	30	pelite	*		*		*	*		I/S		Cent. Chain	0.22	Kln
MF3102	20°58'12"	165°11'49"	20	pelite	*		*	*	*					Cent. Chain	0.19	0.18
MF3103	20°58'00"	165°11'38"	20	pelite	*	*	*	*					Lws	Cent. Chain	0.19	0.16
MF3105	20°52'10"	165°14'40"	60	pelite	*	*	*	*			*			Cent. Chain	0.14	0.21
MF3108	20°52'36"	165°14'18"	20	pelite	*		*	*	*					Cent. Chain	0.29	0.16
MF3110	20°53'18"	165°13'58"	20	pelite	*	*	*		*	*				Cent. Chain	0.49	Kln
MF3115	20°53'18"	165°10'12"	10	pelite	*	*	*	*					Lws+Ep	Boghen	0.16	0.14
MF3118	20°55'12"	165°04'52"	110	pelite	*	*	*	*	*				Lws+Ep	Boghen	0.18	0.17
MF3119	21°19'59"	165°38'51"	20	pelite	*		*		*					Senonian	0.49	-
MF3120	21°20'18"	165°39'03"	40	pelite	*		*			*				Senonian	1.13	Kln
MF3121	21°20'28"	165°39'23"	40	pelite	*	*	*		*	*				Senonian	0.74	Kln
MF3122	21°20'52"	165°40'02"	140	pelite	*		*	*	*			C/S		Senonian	0.43	Kln
MF3123	21°21'32"	165°40'32"	340	pelite	*	*	*	*	*					Senonian	0.43	Kln

MF3125	21°29'32"	165°47'50"	140	pelite	*	*	*	*			I/S		Senonian	0.52	-
MF3126	21°17'53"	165°34'48"	30	pelite	*		*		*	*	I/S		Senonian	0.93	Kln
MF3127	21°17'28"	165°33'10"	40	pelite	*	*	*			*			Cent. Chain	0.17	Kln
MF3128	21°17'19"	165°32'53"	20	pelite	*	*	*	*					Cent. Chain	0.19	0.22
MF3129	21°17'38"	165°31'56"	40	pelite	*		*	*	*				Cent. Chain	0.20	0.20
MF3130	21°18'00"	165°28'41"	40	pelite	*	*	*	*	*				Cent. Chain	0.24	0.18
MF3131	21°18'30"	165°27'31"	40	pelite	*		*	*	*				Cent. Chain	0.20	0.26
MF3132	21°19'42"	165°26'48"	50	marl	*	*	*	*				Ep+Cal	Boghen	0.23	0.21
MF3133	21°22'49"	165°26'11"	180	marl	*	*	*	*				Ep+Cal+Gln	Boghen	0.22	0.18
MF3135	21°23'15"	165°24'24"	120	pelite	*	*	*	*					Boghen	0.21	0.21
MF3136	21°01'32"	165°22'12"	40	pelite	*	*	*	*			C/S	Lws	Cent. Chain	0.20	-
MF3137	21°01'38"	165°21'55"	60	pelite	*	*	*	*				Lws	Cent. Chain	0.17	0.15
MF3138	21°02'43"	165°17'42"	5	pelite	*	*	*	*				Lws	Cent. Chain	0.15	0.14

Mineral abbreviations are from Kretz (1983); except: KWM = K-white micas (illite-muscovite). ML = mixed-layer; I/S = illite/smectite.

C/S = chlorite/smectite. K/S = kaolinite/smectite.

Table 1: (continued)

Sample	Latitude	Longitude	Alt in m.	Rock type	Qtz	Ab	Ms	Chl	Pg	Kln	Stp	ML	others	Terrane	IC	ÁI
PS28	20°57'20"	165°13'50"	10	pelite	*	*	*	*						Cent. Chain	0.18	0.15
PS35	20°56'42"	165°19'32"	20	pelite	*	*	*	*						Cent. Chain	0.19	0.17
PS36	20°57'09"	165°19'48"	10	pelite	*	*	*	*					Lws	Cent. Chain	0.18	0.27
PS37	20°58'30"	165°20'52"	80	pelite	*	*	*	*			*			Cent. Chain	0.14	0.14
PS38	21°04'41"	165°22'48"	20	pelite	*	*	*	*						Cent. Chain	0.22	0.18
PS39	21°04'59"	165°20'42"	5	tuff	*	*	*	*						Cent. Chain	0.20	0.15
PS40	21°04'59"	165°20'42"	5	tuff	*	*	*	*						Cent. Chain	0.26	0.17
PS41	21°04'48"	165°20'28"	40	tuff	*	*	*	*			*			Cent. Chain	0.19	0.16
PS44	21°06'10"	165°19'26"	10	tuff	*	*	*	*			*			Cent. Chain	0.19	0.16
PS45	21°06'19"	165°18'20"	40	tuff	*	*	*	*			*			Cent. Chain	0.24	0.16
PS46b	21°06'03"	165°17'51"	80	tuff	*	*	*	*						Cent. Chain	0.19	0.16
PS47	21°05'55"	165°17'48"	90	pelite	*		*	*	*					Cent. Chain	-	0.15
PS48	21°08'32"	165°27'00"	5	pelite	*	*	*	*						Cent. Chain	0.23	0.33
PS49	21°08'45"	165°25'56"	25	pelite	*	*	*	*			*			Cent. Chain	0.17	0.20
PS50	21°09'20"	165°25'38"	3	marl	*	*	*	*			*		Cal	Cent. Chain	0.28	0.24
PS51	21°09'20"	165°25'38"	3	marl	*	*	*	*			*		Cal	Cent. Chain	0.22	0.21
PS52	21°11'32"	165°26'38"	40	pelite	*	*	*	*						Cent. Chain	0.23	0.29
PS53	21°10'23"	165°23'38"	20	pelite	*	*	*	*						Cent. Chain	0.23	0.19
PS54	21°02'08"	165°21'02"	5	pelite	*		*	*						Cent. Chain	0.19	0.17
PS55	21°02'28"	165°20'54"	20	pelite	*	*	*	*						Cent. Chain	0.15	0.15
PS56b	21°02'33"	165°21'56"	5	pelite	*	*	*	*						Cent. Chain	0.20	0.19
PS57	21°00'02"	165°19'58"	20	pelite	*	*	*	*			*			Cent. Chain	0.23	0.19
PS58	21°09'52"	165°27'53"	20	pelite	*	*	*	*						Cent. Chain	0.20	0.20
PS59	21°10'11"	165°27'39"	25	pelite	*	*	*	*						Cent. Chain	0.23	0.24
PS60	21°10'23"	165°27'22"	20	pelite	*	*	*	*						Cent. Chain	0.22	0.24
PS61	21°10'58"	165°26'41"	20	pelite	*	*	*	*						Cent. Chain	0.19	0.20
PS62	21°11'31"	165°26'38"	20	pelite	*	*	*	*						Cent. Chain	0.23	0.18
PS63	21°22'48"	165°40'31"	120	pelite	*	*	*	*						Cent. Chain	0.14	0.19
PS64	21°23'03"	165°40'25"	120	marl	*	*	*	*					Cal	Cent. Chain	0.18	0.17

PS66	21°23'29"	165°39'40"	60	marl	*	*	*	*			Cal	Cent. Chain	0.18	0.19
PS67	21°23'28"	165°39'28"	70	pelite	*	*	*	*			Lws	Cent. Chain	0.18	0.20
PS68	21°23'28"	165°39'28"	70	pelite	*	*	*	*			Lws	Cent. Chain	0.17	0.19
PS69	21°22'48"	165°38'23"	110	pelite	*	*	*	*		*		Cent. Chain	0.16	0.17
PS70	21°22'58"	165°38'41"	95	pelite	*	*	*	*				Cent. Chain	0.21	0.18
PS71	21°23'49"	165°39'00"	80	pelite	*	*	*	*			Ep+Cal	Boghen	0.15	0.14
PS72	21°24'25"	165°38'41"	80	pelite	*		*	*				Boghen	-	0.28
PS73	21°24'41"	165°38'19"	90	pelite	*	*	*	*			Lws	Boghen	0.21	0.17
PS74	21°25'30"	165°38'12"	100	pelite	*	*	*	*				Boghen	0.15	0.15
PS75	21°25'52"	165°38'08"	100	pelite	*	*	*	*			Cal	Boghen	0.15	0.14
PS77	21°20'20"	165°26'25"	40	pelite	*	*	*	*			Ep+Cal	Boghen	0.14	0.15
PS78	21°20'50"	165°25'32"	80	pelite	*	*	*	*			Ep	Boghen	0.13	0.13
PS79	21°21'08"	165°25'31"	85	pelite	*	*	*	*			Ep+Cal	Boghen	0.20	0.17
PS82	21°23'21"	165°24'20"	160	pelite	*	*	*	*				Boghen	0.15	0.13
PS84	21°22'40"	165°25'59"	180	pelite	*	*	*	*			Gln+Cal	Boghen	0.12	0.14
PS85	21°22'42"	165°26'00"	200	pelite	*	*	*	*			Gln+Ep	Boghen	0.23	0.15

Mineral abbreviations are from Kretz (1983); except: KWM = K-white micas (illite-muscovite). ML = mixed-layer; I/S = illite/smectite.

C/S = chlorite/smectite. K/S = kaolinite/smectite.

Table 2: Representative chemical analyses of K-white micas.

Sample N°	PS46b		PS54		PS56b		PS69		PS85	
n	11	SD	18	SD	17	SD	12	SD	7	SD
SiO_2	50.33	0.57	50.48	0.98	49.72	0.74	51.90	0.55	52.55	0.63
TiO_2	0.10	0.09	0.06	0.06	0.05	0.06	0.13	0.14	0.14	0.18
Al_2O_3	28.14	1.09	23.10	0.68	24.56	1.05	23.75	0.69	23.48	0.41
FeO	3.78	0.42	2.80	0.81	4.82	0.68	4.63	0.47	4.20	0.41
MnO	0.09	0.08	0.05	0.06	0.07	0.05	0.05	0.06	0.06	0.05
MgO	2.06	0.37	4.49	0.48	2.78	0.47	4.63	0.23	4.31	0.24
CaO	0.06	0.07	0.02	0.02	0.04	0.03	0.05	0.04	0.09	0.10
Na_2O	0.10	0.06	0.06	0.02	0.11	0.28	0.12	0.16	0.09	0.03
K_2O	9.86	0.10	10.41	0.56	10.77	0.26	11.03	0.27	11.44	0.38
Total	94.52	0.42	91.47	0.73	92.91	0.66	95.56	0.77	96.35	0.56
Si	3.39	0.04	3.52	0.03	3.46	0.05	3.50	0.03	3.52	0.03
Ti	0.00	0.00	0.00	0.00	0.00	0.00	0.01	0.01	0.01	0.01
Al^{IV}	0.61	0.04	0.48	0.03	0.54	0.05	0.50	0.03	0.48	0.03
Al^{VI}	1.62	0.04	1.42	0.05	1.47	0.04	1.39	0.03	1.37	0.03
Fe^{2+}	0.21	0.02	0.16	0.05	0.28	0.04	0.26	0.03	0.23	0.02
Mn	0.00	0.00	0.00	0.00	0.00	0.00	0.00	0.00	0.00	0.02
Mg	0.21	0.04	0.47	0.05	0.29	0.05	0.39	0.02	0.43	0.03
Ca	0.00	0.01	0.00	0.00	0.00	0.00	0.00	0.00	0.01	0.01
Na	0.01	0.01	0.01	0.00	0.01	0.01	0.02	0.02	0.01	0.00
K	0.85	0.01	0.93	0.05	0.96	0.02	0.95	0.02	0.98	0.03
t.i.c.	0.86	0.01	0.94	0.05	0.97	0.02	0.97	0.02	1.00	0.02
b_0	9.04		9.05		9.05		9.05		9.06	
KI	0.25		0.25		0.26		0.21		0.30	

Calculations are based on 11 oxygens (anhydrous basis). SD: standard deviation. b_0 values calculated after Guidotti et al. (1989). t.i.c = total interlayer cations (Ca+Na+K).

Table 3: Representative chemical analyses of chlorite.

Sample N°	MF3100		MF3128		PS46b		PS54		PS56b		PS81*	
n	13	SD	17	SD	8	SD	7	SD	7	SD	5	SD
SiO_2	29.29	0.43	25.68	0.41	26.09	0.42	28.42	0.65	25.06	0.49	26.16	0.55
TiO_2	0.01	0.03	0.04	0.06	0.06	0.05	0.06	0.03	0.11	0.11	0.09	0.13
Al_2O_3	20.54	0.20	17.33	0.39	19.41	0.14	17.20	0.35	19.17	0.49	18.19	0.57
FeO	3.79	1.01	31.76	0.60	30.41	0.43	19.96	0.32	32.19	0.53	28.29	1.24
MnO	0.27	0.04	0.64	0.06	0.43	0.08	0.57	0.11	0.50	0.09	0.49	0.07
MgO	29.45	0.74	9.98	0.36	10.87	0.31	19.35	0.37	9.39	0.22	13.82	0.51
CaO	0.05	0.02	0.13	0.04	0.08	0.16	0.03	0.02	0.05	0.04	0.18	0.11
Na_2O	0.01	0.01	0.01	0.01	0.03	0.03	0.01	0.01	0.04	0.03	0.05	0.04
K_2O	0.02	0.02	0.05	0.02	0.03	0.03	0.03	0.05	0.14	0.07	0.02	0.02
Total	83.42	0.76	85.63	0.77	87.40	0.81	85.62	0.73	86.66	0.78	87.29	1.12
Si	5.76	0.05	5.79	0.07	5.68	0.04	5.96	0.09	5.58	0.10	5.65	0.09
Ti	0.00	0.00	0.01	0.01	0.01	0.01	0.01	0.01	0.02	0.02	0.01	0.01
Al^{IV}	2.24	0.05	2.21	0.07	2.32	0.04	2.04	0.09	2.42	0.10	2.35	0.09
Al^{VI}	2.53	0.03	2.39	0.06	2.65	0.03	2.22	0.07	2.62	0.05	2.29	0.08
Fe^{2+}	0.62	0.17	5.99	0.12	5.53	0.09	3.50	0.05	5.99	0.08	5.11	0.22

Mn	0.04	0.01	0.12	0.01	0.08	0.02	0.10	0.02	0.09	0.02	0.09	0.01
Mg	8.64	0.20	3.35	0.11	3.53	0.07	6.06	0.11	3.19	0.08	4.45	0.18
Ca	0.01	0.01	0.03	0.01	0.02	0.04	0.01	0.01	0.01	0.01	0.04	0.03
Na	0.00	0.00	0.00	0.01	0.01	0.01	0.00	0.00	0.02	0.01	0.02	0.02
K	0.01	0.00	0.02	0.01	0.01	0.01	0.01	0.01	0.04	0.02	0.01	0.00
$Fe^{2+}/(Fe^{2+}+Mg)$	0.07	0.02	0.64	0.01	0.61	0.01	0.37	0.01	0.66	0.01	0.53	0.02
T (°C)	298	8	294	11	312	7	266	15	327	16	316	15

Calculations are based on 28 oxygens (anhydrous basis). SD: standard deviation. All Fe is assumed to be Fe^{2+}. Temperatures are determined using the chlorite thermometer of Cathelineau (1988). (*) Sample PS81 is a metabasite, others are pelites.

Figure 1

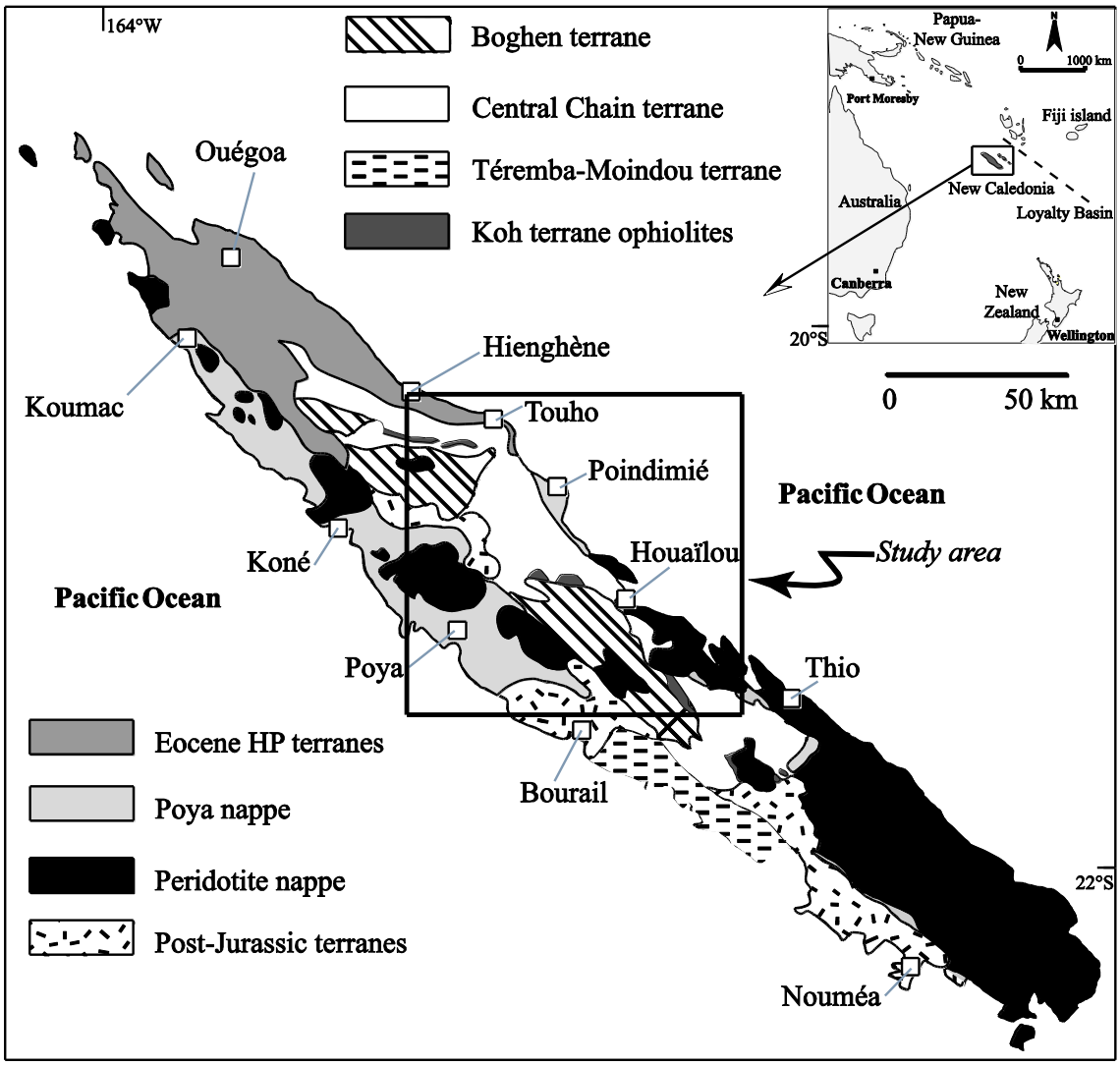
164°W
Boghen terrane
Central Chain terrane
Téremba-Moindou terrane
Koh terrane ophiolites
Papua-
New Guinea
N
0
1000 km
Port Moresby
Fiji island
Australia
New Caledonia
Loyalty Basin
Canberra
New
Zealand
Wellington
20°S
0
50 km
Ouégoa
Koumac
Hienghène
Touho
Poindimié
Houaïlou
Koné
Pacific Ocean
Pacific Ocean
Study area
Poya
Thio
Bourail
Eocene HP terranes
Poya nappe
Peridotite nappe
Post-Jurassic terranes
22°S
Nouméa

Figure 2

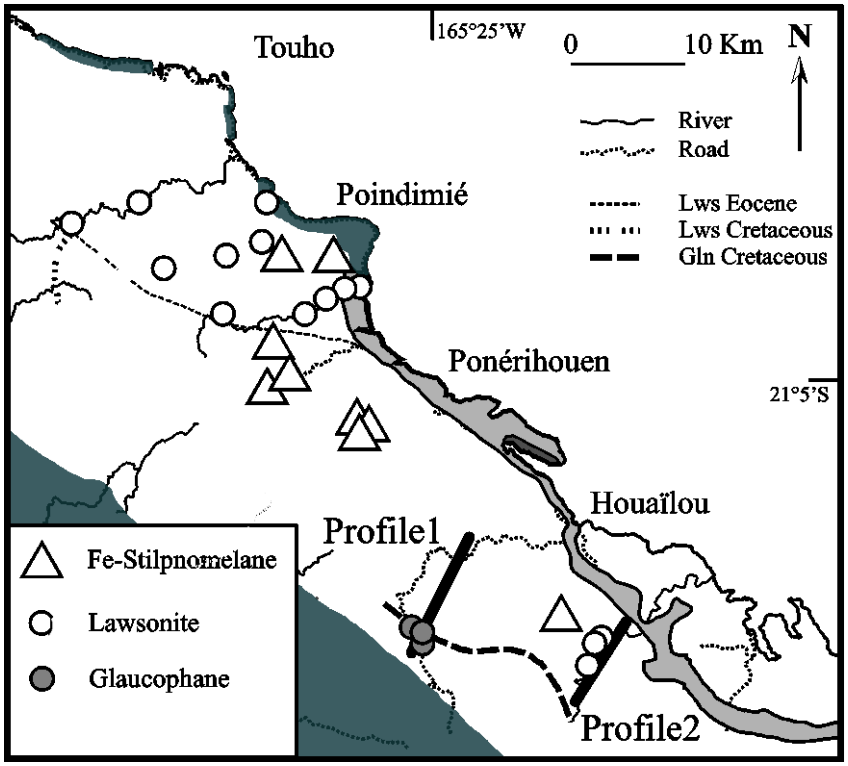

Figure 3

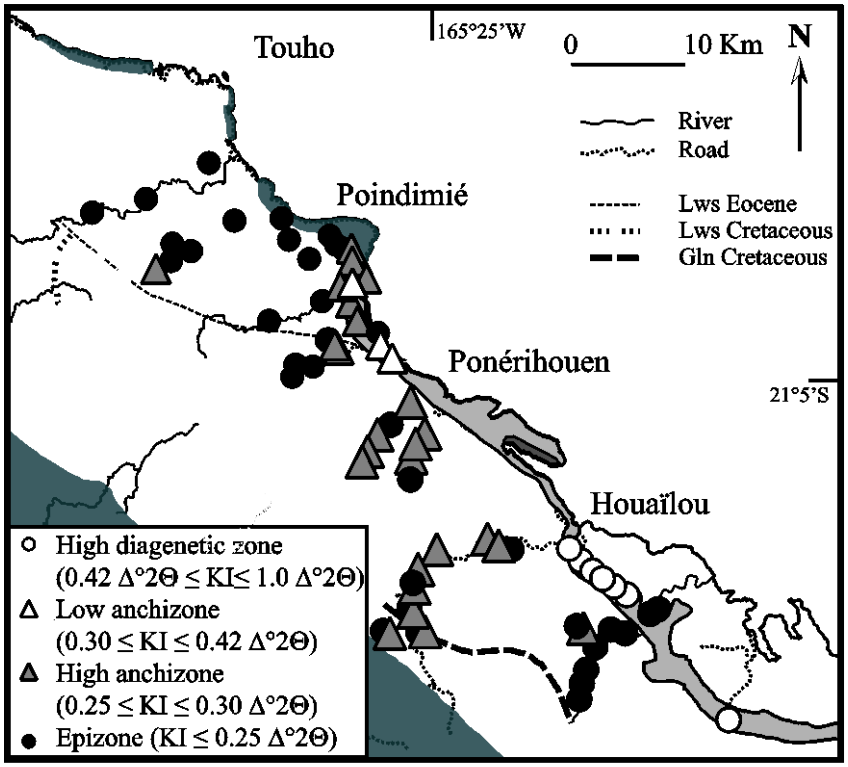

Figure 4

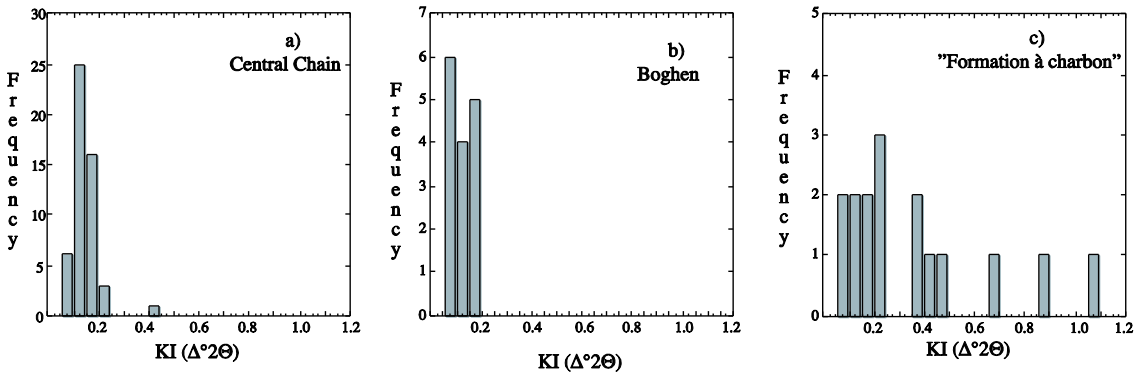

Figure 5

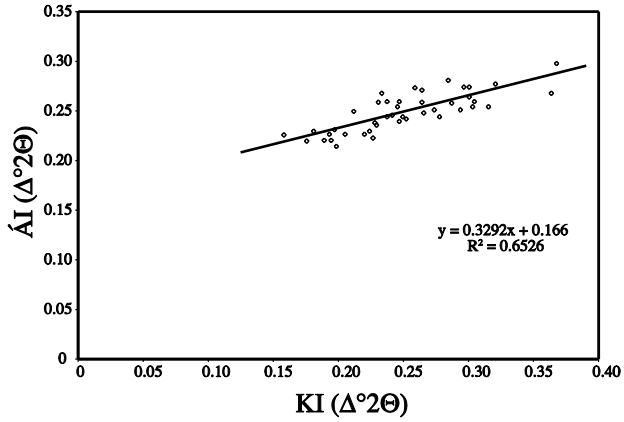

Figure 6

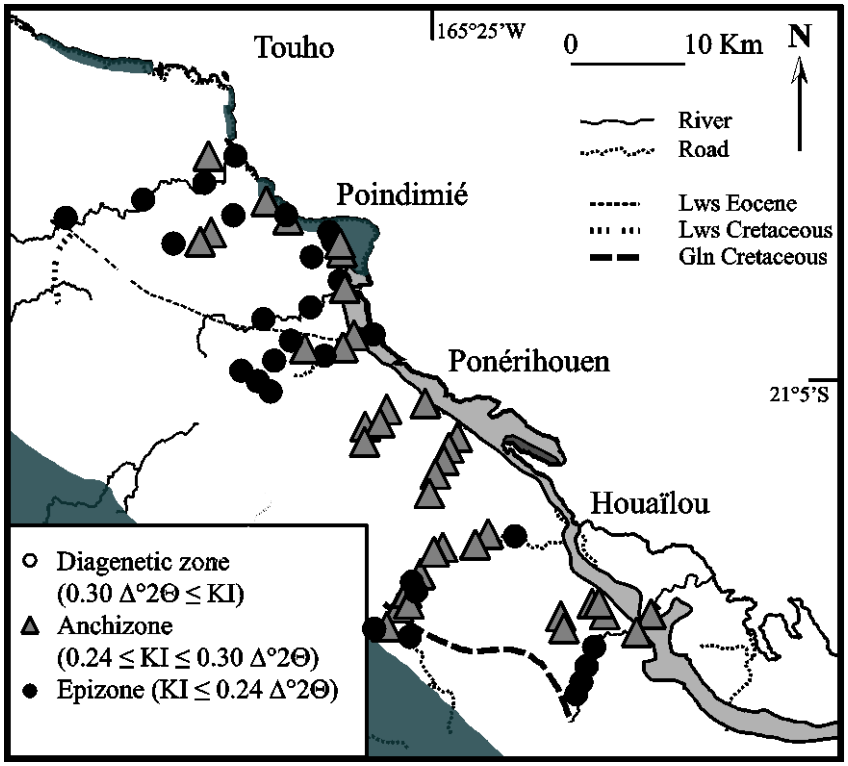
Touho
165°25'W
0
10 Km
N
River
Road
Lws Eocene
Lws Cretaceous
Gln Cretaceous
Poindimié
Ponérihouen
21°5'S
Houaïlou
Diagenetic zone
(0.30 Δ°2Θ ≤ KI)
Anchizone
(0.24 ≤ KI ≤ 0.30 Δ°2Θ)
Epizone (KI ≤ 0.24 Δ°2Θ)

Figure 7

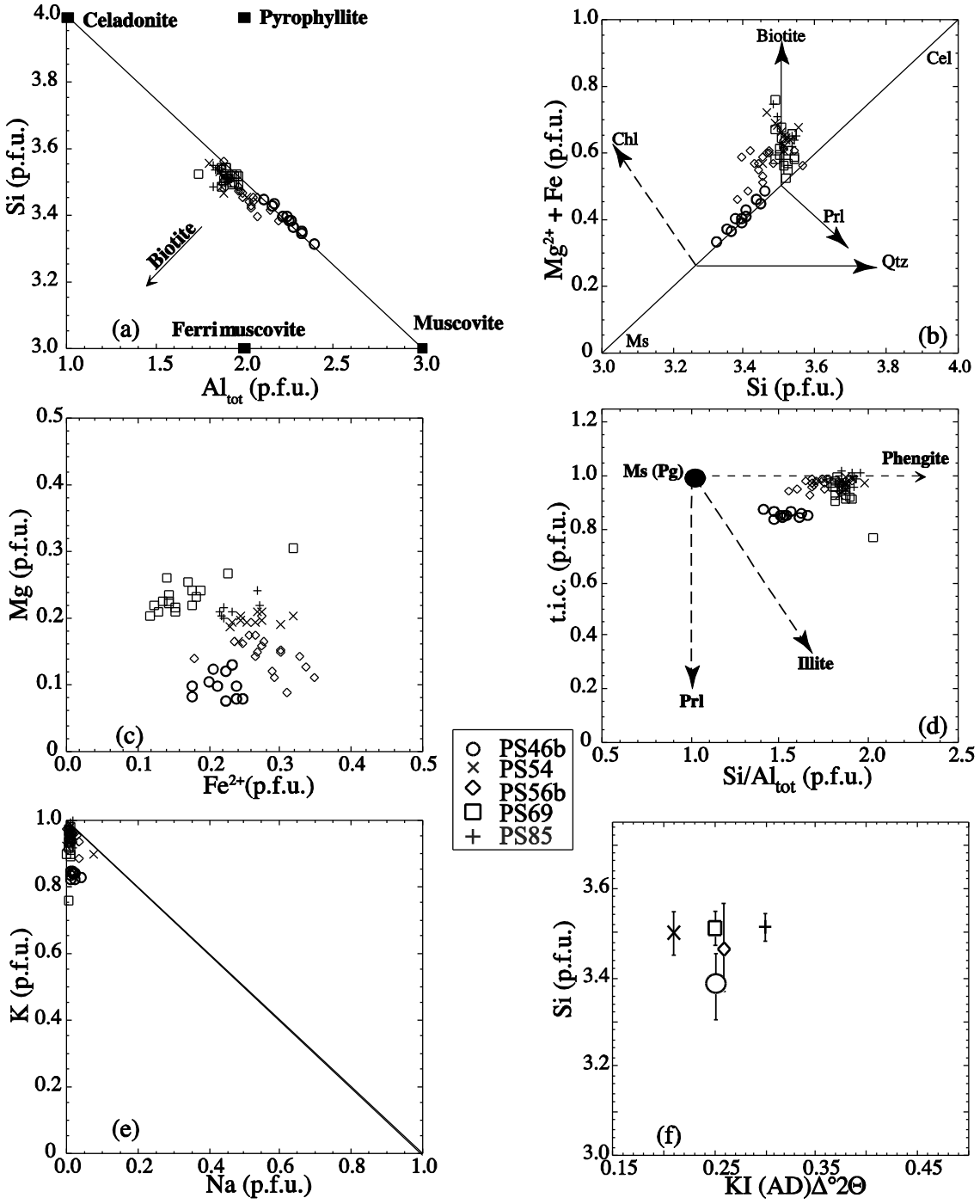
Celadonite
Pyrophyllite
Biotite
(a)
Ferrimuscovite
Muscovite
Si (p.f.u.)
Al$_{tot}$ (p.f.u.)
Biotite
Cel
Chl
Prl
Qtz
Ms
(b)
Mg^{2+} + Fe (p.f.u.)
Si (p.f.u.)
Mg (p.f.u.)
Fe^{2+}(p.f.u.)
(c)
Ms (Pg)
Phengite
Illite
Prl
(d)
t.i.c. (p.f.u.)
Si/Al$_{tot}$ (p.f.u.)
PS46b
PS54
PS56b
PS69
PS85
K (p.f.u.)
Na (p.f.u.)
(e)
Si (p.f.u.)
(f)
KI (AD)Δ°2Θ

Figure 8

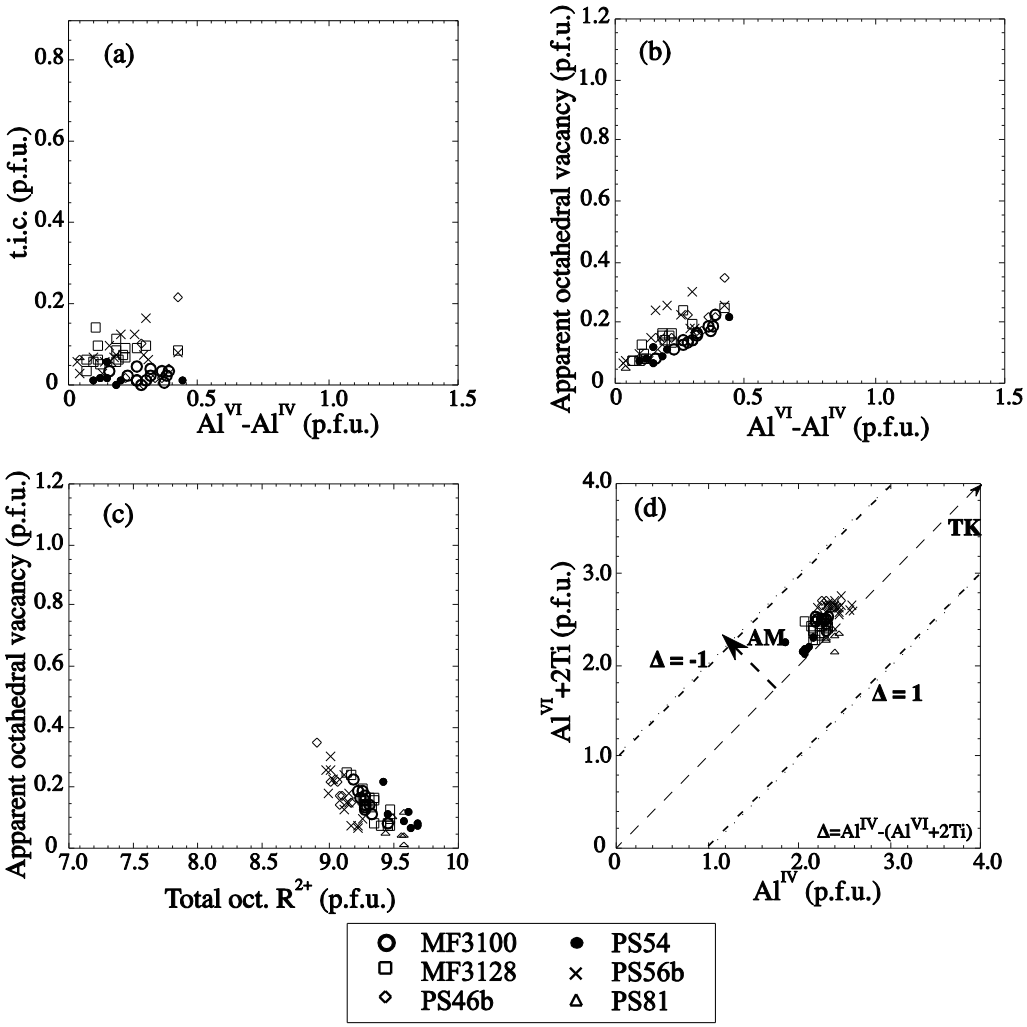
(a)
t.i.c. (p.f.u.)
Al^{VI}-Al^{IV} (p.f.u.)
(b)
Apparent octahedral vacancy (p.f.u.)
Al^{VI}-Al^{IV} (p.f.u.)
(c)
Apparent octahedral vacancy (p.f.u.)
Total oct. R^{2+} (p.f.u.)
(d)
TK
AM
Δ = -1
Δ = 1
Δ=Al^{IV}-(Al^{VI}+2Ti)
Al^{VI}+2Ti (p.f.u.)
Al^{IV} (p.f.u.)
MF3100
MF3128
PS46b
PS54
PS56b
PS81

Figure 9

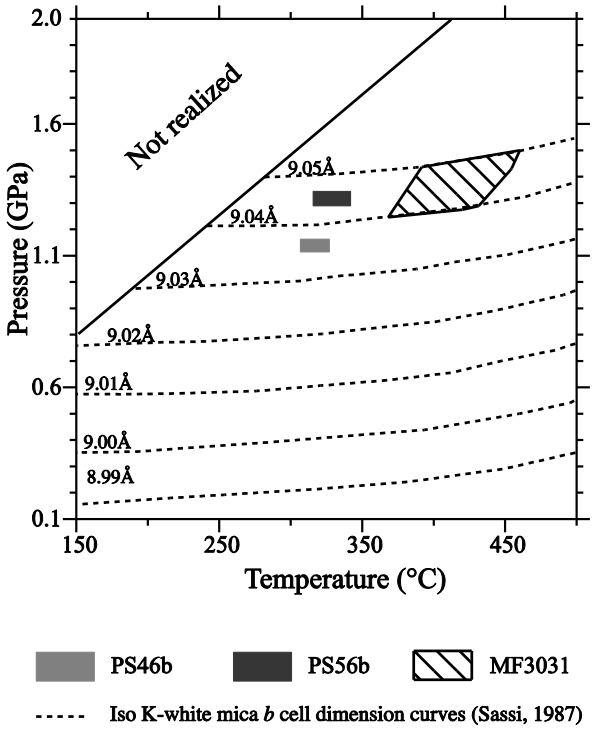

Figure 10

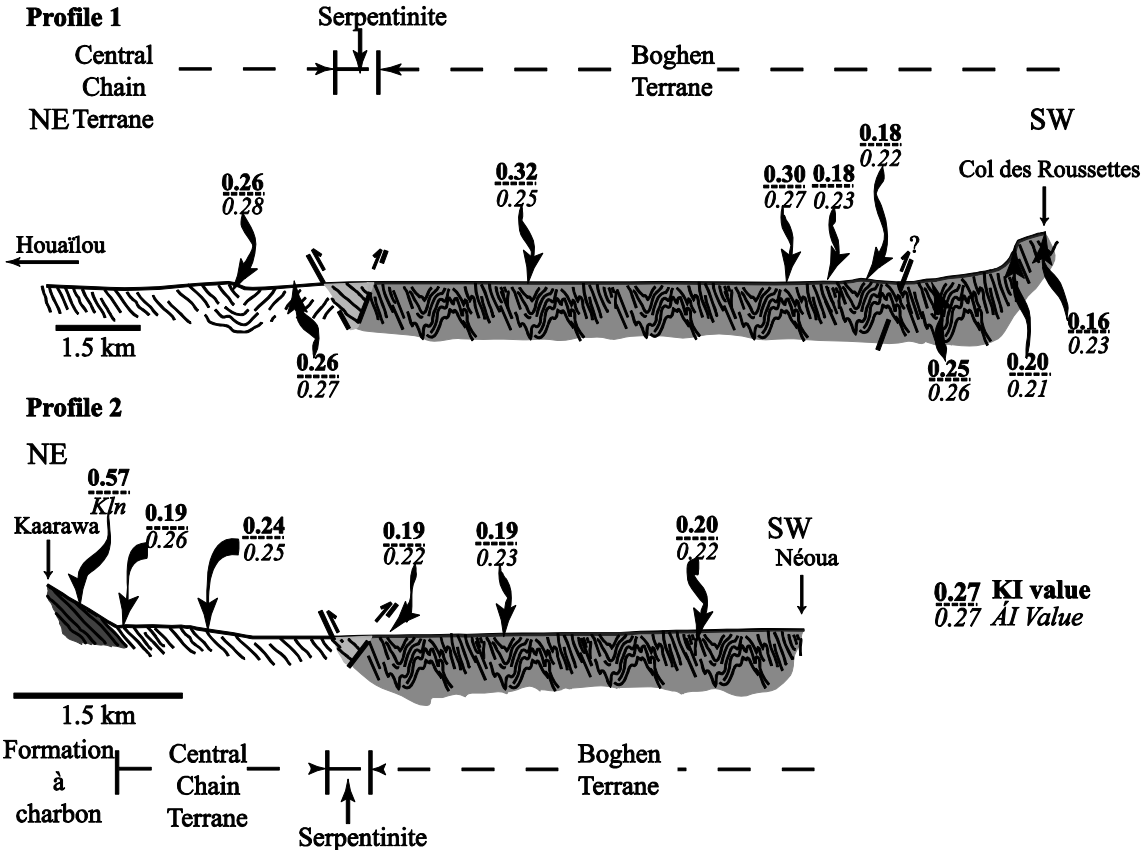

Figure 11

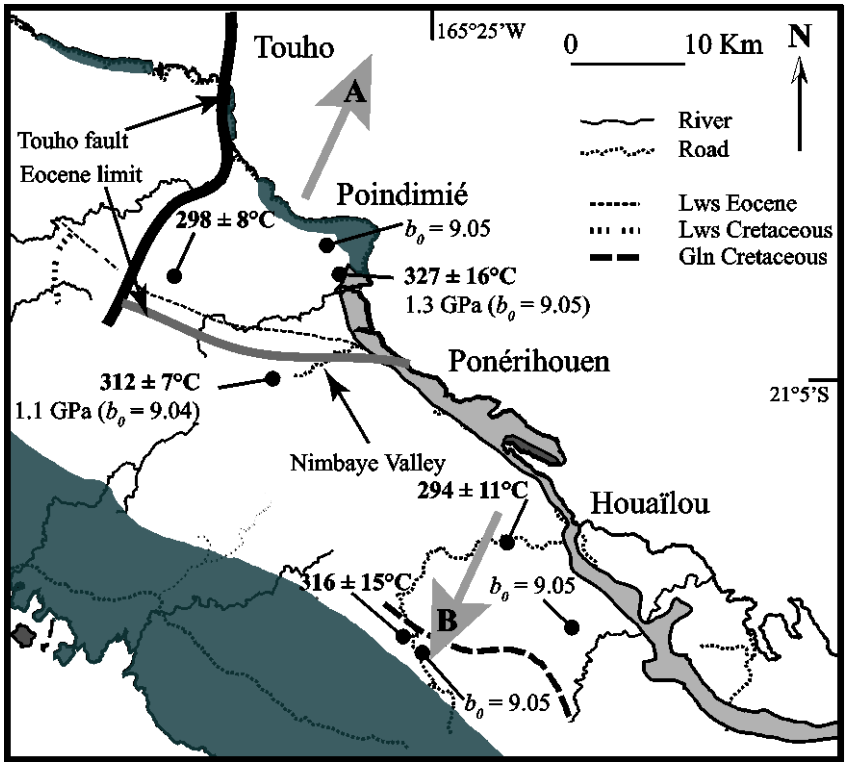
Touho
165°25'W
0
10 Km
N
A
River
Road
Touho fault
Eocene limit
Poindimié
298 ± 8°C
b_0 = 9.05
Lws Eocene
Lws Cretaceous
Gln Cretaceous
327 ± 16°C
1.3 GPa (b_0 = 9.05)
Ponérihouen
312 ± 7°C
1.1 GPa (b_0 = 9.04)
21°5'S
Nimbaye Valley
294 ± 11°C
Houaïlou
316 ± 15°C
b_0 = 9.05
B
b_0 = 9.05